Chapter

Photodynamic Inactivation of *Escherichia coli* with Cationic Porphyrin Sensitizers

Jin Matsumoto, Tomoko Matsumoto, Kazuya Yasuda and Masahide Yasuda

Abstract

The activity of singlet-oxygen sensitizers for photodynamic inactivation (PDI) of microorganisms and photodynamic therapy of tumor cells has been evaluated using *Escherichia coli*, *Saccharomyces cerevisiae*, and human cancer cell lines. In this chapter, drug resistance of *E. coli* was examined based on the PDI activity of a variety of RPy-P-porphyrin sensitizers with different number of ionic valence and different hydrophobic characters. The PDI activities toward *E. coli* were evaluated using the minimum effective concentrations ($[P]$) of the porphyrin sensitizers. It was found that the $[P]$ value for *E. coli* was larger than that for *S. cerevisiae*. *E. coli* has drug-resistance toward hydrophobic and mono-cationic porphyrins. However, *E. coli* has weak drug-resistance toward the porphyrins with both polycationic character and hydrophobicity. Since the outer membrane mainly consists of lipopolysaccharides and phospholipids that are negatively charged, cationic porphyrins are able to adsorb to the outer leaflet. Then the cationic porphyrins with hydrophobic character can interact with not only the outer leaflet but also inner leaflet of the outer membrane and the plasma membrane. Thus, porphyrins may be incorporated inside *E. coli* cells via the self-promoted uptake pathway. Moreover, polycationic porphyrins can interact with DNA and proteins by strong binding affinities.

Keywords: PDT sensitizer, singlet oxygen, porphyrins, PDI activity, *Escherichia coli*, *Saccharomyces cerevisiae*

1. Introduction

Singlet-oxygen ($^1O_2$) sensitizers for photodynamic inactivation (PDI) of microorganisms and photodynamic therapy of tumor cells have been developed using *Escherichia coli*, *Saccharomyces cerevisiae*, and human cancer cell lines (e.g., HeLa cell) as model cells [1–4]. As *E. coli* is a Gram-negative bacterium, the cell wall consists of an inner membrane, cytoplasmic membrane, a periplasmic space with a peptidoglycan layer, and an outer membrane [5]. Since the *E. coli* cell wall has a low permeability, there are only a few $^1O_2$-sensitizers that can permeate the cell wall and inactivate
E. coli efficiently at low concentrations.

PDI refers to the use of a visible-light source, oxidizing agents (e.g., O_2), and photosensitizers. Photosensitizers absorb light energy that causes an energy transfer
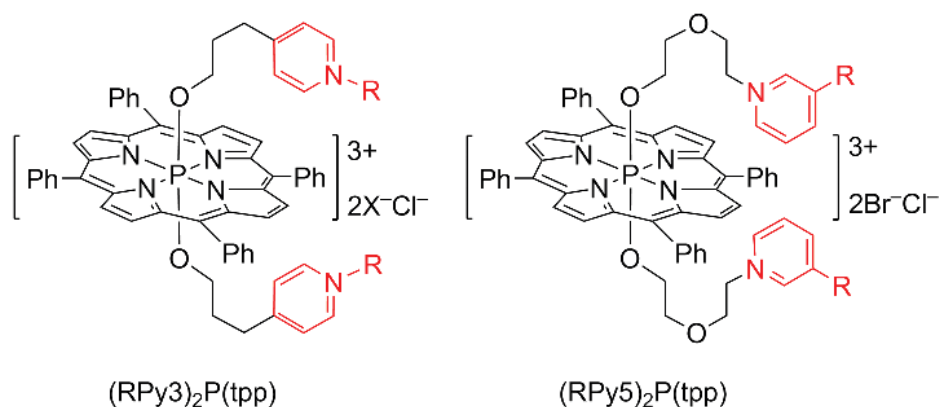
Figure 1.
Typical structure of porphyrin sensitizer (P type).

to O_2, which leads to the formation of reactive oxygen such as $^1O_2$, thereby inactivating cells and bacteria. Preliminary studies on the photodynamic action for biological systems started in the 1930s by PDI of phages using methylene blue [6, 7]. PDI of bacteria has received considerable attention as a methodology leading to the medical application of infection therapy beyond antimicrobial resistance. Among the large variety of photosensitizers developed for PDI over the last 60 years, porphyrins and metalloporphyrins became attractive sensitizers owing to their strong absorption band in the visible-light region [8–11].

In the case of porphyrin sensitizers, their solubilities in water are an important characteristic for handling them as aqueous solutions, since porphyrin derivatives, in general, are poorly soluble in water. The most popular method to improve the solubility in water is the introduction of ionic groups to the porphyrin ring. Especially, the introduction of an alkylpyridinium (RPy) group into porphyrins is a useful method to make porphyrins water-soluble [12, 13]. A typical RPy-bonded porphyrin is represented by *meso*-tetra[4-(1-methyl-pyridinium)] porphyrin (TMP). The first application of TMP to PDI was reported by Ben Amor et al. in 1998 [14]. For the last two decades, a variety of RPy-bonded porphyrins have been prepared and studied for PDI [15–21].

We have interested in axially RPy-bonded tricationic P-porphyrins and their PDI activity [22–26]. It is advantageous that the water solubilization is easily achieved through the modification of the axial ligands of P-porphyrins. It is expected that polycationic porphyrins have strong binding affinities to DNA [27–32]. In this chapter, drug resistance of *E. coli* was discussed based on PDI activity of a variety of P- and Sb-porphyrin sensitizers with different number of ionic valence and different hydrophobic character. The typical structure of the porphyrin sensitizer is shown in **Figure 1**, and they are named P-type porphyrin.

2. Materials and methods

2.1 Axially RPy-bonded tricationic P-porphyrins: $(RPy3)_2P(Tpp)^{3+}$

The preparation of tricationic bis[3-(1-alkyl-4-pyridinio)propoxo] tetraphenylporphyrinatophosphorus(V) complex, $(RPy3)_2P(Tpp)^{3+}$ (Tpp = tetraphenylporphyrinato group), was performed as follows [22]. Dichloro(tetraphenylporphyrinato)phosphorus chloride ([$Cl_2P(Tpp)$]Cl [33], 300 mg) was reacted with 3-(4-pyridyl)-1-propanol (5.0 mL) in MeCN (30 mL) at reflux temperature

for about 24 h until the Soret band shifted from 435 to 428 nm. Bis[3-(4-pyridyl)propoxo]tetraphenylporphyrinatophosphorus(V) chloride, $(Py3)_2P(Tpp)^+$, was produced in 47% yield. The $(Py3)_2P(Tpp)^+$ (50 mg) was reacted with alkyl halides (1.0 mL) in MeCN (25 mL) at reflux temperature for about 24 h to give $(RPy3)_2P(Tpp)^{3+}$ [22]. The yields of $(RPy3)_2P(Tpp)^{3+}$ are listed in **Table 1**.

2.2 Axially RPy-bonded polycationic Sb-porphyrins

Axially RPy-bonded polycationic Sb-porphyrins were prepared using dibromo(tetraphenylporphyrinato)antimony bromide ($[Br_2Sb(Tpp)]Br$) as the starting material [34]. The partial methanolysis of $[Br_2Sb(Tpp)]Br$ (1.077 g) was performed in MeOH-MeCN (1:1, 160 mL) in the presence of pyridine (0.75 mL) at 80°C until the Soret band shifted from 427 to 423 nm. Bromo(methoxo)-(tetraphenylporphyrinato)antimony bromide ($[MeO(Br)Sb(Tpp)]Br$, 520 mg) was formed in 61% yield [35]. An MeCN (20 mL) solution of $[Br_2Sb(Tpp)]Br$ (150 mg) and $[MeO(Br)Sb(Tpp)]Br$ (180 mg) was heated with 3-(4-pyridyl)-1-propanol (3.7 mL) at refluxing temperature for about 24 h until the Soret band

Sensitizers	n [b]	Z [a]	Metal	Yield /%	$\varepsilon/10^4 \ M^{-1} \ cm^{-1}$ [c]		C_W/mM [d]
					Soret	Q	
$(MePy3)_2P(tpp)$	1	+3	P	95	26.9	1.38	3.4
$(BuPy3)_2P(tpp)$	4	+3	P	93	23.1	1.18	6.1
$(PentPy3)_2P(tpp)$	5	+3	P	32	27.2	1.32	3.8
$(HexPy3)_2P(tpp)$	6	+3	P	47	31.3	1.45	5.8
$(HeptPy3)_2P(tpp)$	7	+3	P	32	26.7	1.26	6.0
$(OctPy3)_2P(tpp)$	8	+3	P	48	18.7	0.97	3.8
$(HexPy3)_2Sb(tpp)$	6	+3	Sb	35	16.3	4.18	11.1
$(MePy3)Sb(tpp)$	1	+2	Sb	42	12.7	4.45	2.4
$(HexPy3)Sb(tpp)$	6	+2	Sb	25	15.1	4.48	5.2
$(MePy5)_2P(tpp)$	1	+3	P	73	28.2	1.36	>120
$(EtPy5)_2P(tpp)$	2	+3	P	58	29.6	1.40	>120
$(ButPy5)_2P(tpp)$	4	+3	P	44	25.3	1.29	112
$(HexPy5)_2P(tpp)$	6	+3	P	44	24.7	1.22	64
$(4EtPy5)_2P(tpp)$	2	+3	P	72	12.7 [e]	0.57 [e]	>120
$(Me)_2P(PyHex)$	6	+2	P	57	22.6	1.31	5.0
$(Me1)_2P(PyHex)$	6	+2	P	78	14.1	0.89	11.4
$(Bu1)_2P(PyMe)$	1	+2	P	94	18.1	1.01	13.6
$(Bu2)_2P(PyMe)$	1	+2	P	32	21.7	1.21	13.0
$(Hex2)_2P(PyMe)$	1	+2	P	45	28.6	1.63	8.0

[a] *Z = charge of the complex.*
[b] *n = carbon number of the alkyl chain on the Ap.*
[c] *Molar absorption coefficient for the Soret and the Q bands in MeOH solution.*
[d] *C_W = water solubility in mM.*
[e] *Broadening of UV spectra occurred.*

Table 1.
PDI of E. coli with cationic porphyrins.

shifted to 418 nm, respectively. Thus, bis[3-(4-pyridyl)propoxo]tetraphenyl-porphyrinatoantimony (V) bromide (($Py3)_2Sb(Tpp)^+$, 83 mg) and 3-(4-pyridyl) propoxo(methoxo)tetraphenylporphyrinatoantimony (V) bromide ($Py3Sb(Tpp)^+$, 90 mg) were obtained in 50% and 43% yields, respectively. $(Py3)_2Sb(Tpp)^+$ (50 mg) was reacted with 1-bromohexane (0.5 mL) in MeCN (13 mL) at reflux temperature for about 24 h to give bis[3-(1-hexyl-4-pyridinio)-1-propoxo]-5,10,15,20-tetraphenylporphyrinatoantimony (V) tribromide (($HexPy3)_2Sb(Tpp)^{3+}$, 20 mg, 35%). The reaction of ($Py3Sb(Tpp)^+$, 50 mg) with MeI and 1-bromohexane (0.5 mL in MeCN (13 mL) at reflux temperature for about 24 h gave α-(methoxo)-β-[3(1--methyl-4-pyridinio)-1-propoxo]-5,10,15,20-tetraphenylporphyrinatoantimony (V) dibromide ($MePy3Sb(Tpp)^{2+}$, 25 mg, 42%) and α-(methoxo)-β-[3 (1-hexyl-4-pyridinio)-1-propoxo]-5,10,15,20-tetraphenyl-porphyrinatoantimony (V) dibromide ($HexPy3Sb(Tpp)^{2+}$, 20 mg, 25%), respectively [24].

2.3 Axially RPy-bonded tricationic P-porphyrins: $(RPy5)_2P(Tpp)^{3+}$

Bis[5-(3-alkyl-1-pyridinio)-3-oxapentyloxo]tetraphenylporphyrinato-phosphorus(V) dibromide, chloride (($RPy5)_2P(Tpp)^{3+}$) was prepared from dihydroxo(tetraphenylporphyrinato)phosphorus chloride ($[(HO)_2P(Tpp)]Cl$), which was prepared by hydrolysis of $[Cl_2P(Tpp)]Cl$ (300 mg) by refluxing in a mixed solvent of MeCN (160 mL) with pyridine (60 mL) and H_2O (60 mL) [22]. Alkylation of $[(HO)_2P(Tpp)]Cl$ (80 mg) with di(2-bromoethyl) ether (1 mL) was performed in the presence of K_2CO_3 (19 mg) and 18-crown-6 ether (4.2 mg) in MeCN (5 mL) at 50°C to give bis(5-bromo-3-oxa-pentyloxo)tetraphenyl-porphyrinatophosphorus(V) chloride (($Br5)_2P(Tpp)^+$). The $(Br5)_2P(Tpp)^+$ (50 mg) was reacted with 3-alkylpyridine (1.0 mL) in MeCN (10 mL) under heating at 100°C for 20–68 h for the preparations of $(RPy5)_2P(Tpp)^{3+}$ [22]. Similarly, bis[5-(4-ethyl-1-pyridinio)-3-oxapentyloxo]tetraphenylporphyrinatophosphorus(V) dibromide, chloride, $(4EtPy5)_2P(Tpp)^{3+}$ was prepared via the reaction of $(Br5)_2P(Tpp)^+$ (63 mg) with 4-ethylpyridine (1.0 mL) in dry MeCN (10 mL) at 100°C for 20 h.

2.4 RPy-bonded dicationic P-porphyrins at *meso* position: $(R'm)_2P(RPyTpp)^{2+}$

At first, 5,10,15-triphenyl-20-(4-pyridinyl)porphyrin (PyTpp) was prepared by reaction of pyrrole (1.55 mL), benzaldehyde (1.83 mL), and 4-formylpyridine (0.56 mL) in propanoic acid (100 mL) in an oil bath heated at 140°C for 1 h to give PyTpp (533 mg, 14%) [24]. PyTpp (101 mg) was reacted with phosphoryl chloride ($POCl_3$, 2.0 mL) in pyridine (10 mL) in a pressure bottle heated at 180°C for 1 day to give dichloro[triphenyl(4-pyridinyl)porphyrinato]phosphorus chloride ($[Cl_2P(PyTpp)]Cl$, 99.0 mg) in 81% yield. Substitution of the axial chloro ligand with a methoxo group was performed by refluxing $[Cl_2P(PyTpp)]Cl$ (82.7 mg) in MeOH (20 mL)-pyridine (0.25 mL) for 3 days until the Soret band shifted from 435 to 424 nm. Dimethoxo[5-(1-hexyl-4-pyridinio)-10,15,20-triphenyl-porphyrinato] phosphorus (V) dichloride (($Me)_2P(HexPyTpp)^{2+}$) was prepared by reaction of $[(MeO)_2P(PyTpp)]Cl$ (62.0 mg) with 1-iodohexane (2 mL) in DMF (5 mL) in the presence of K_2CO_3 (19 mg) at 100°C for 2 h. $(Me)_2P(HexPyTpp)^{2+}$ was purified through anion exchange with chloride ions, as follows. An aqueous solution (10 mL) of $AgBF_4$ (115 mg) was added to a MeCN-MeOH (1:1 v/v, 20 mL) solution of the porphyrins. After stirring for 24 h at room temperature, the solution was washed with water (100 mL) and an aqueous NaCl solution (100 mL) three times and subjected to precipitation with hexane (200 mL) [24].

4

[Cl$_2$P(PyTpp)]Cl (78–100 mg) was reacted with ethylene glycol derivatives (H(OCH$_2$CH$_2$)$_m$OR', R' = Me, *n*-Bu, *n*-Hex, 5–7 mL) in MeCN (10 mL) in the presence of pyridine (0.75 mL) for 24 h to give bis(2-alkyloxyethoxo)-5-(4-pyridinyl)-10,15,20-triphenylporphyrinatophosphorus (V) chloride ([(R'*m*)$_2$P(PyTpp)]Cl) in 66–88%. Bis(2-methoxyethoxo)-5-(1-hexyl-4-pyridinyl)-10,15,20-triphenylporphyrinatophosphorus (V) bromide, chloride ((Me*1*)$_2$P(HexPyTpp)$^{2+}$) was prepared by reaction of [(Me*1*)$_2$P(PyTpp)]Cl (51 mg) with 1-iodohexane (2 mL) in DMF (5 mL) in the presence of K$_2$CO$_3$ (19 mg) in an oil bath heated at 100°C for 2 h. After anion-exchange, dichloride salt of (Me*1*)$_2$P(HexPyTpp)$^{2+}$ (27 mg, 78%) was obtained. Also, other *meso*-RPy-bonded dicationic P-porphyrins (61–90 mg) were reacted with MeI (1.2 mL) in DMF (7.5 mL) in the presence of K$_2$CO$_3$ (43 mg) by heating at 100°C for 24 h to give an *N*-methyl-substituted complex. After anion exchange, (Me1)$_2$P(HexPyTpp)$^{2+}$ (35 mg, 94%), (Bu*2*)$_2$P(MePyTpp)$^{2+}$ (13.7 mg, 32%), and (Hex*2*)$_2$P(MePyTpp)$^{2+}$ (28.0 mg, 45%) were formed [24].

2.5 Preparation of *E. coli* suspension

E. coli K-12 (IFO 3301) was cultured aerobically at 30°C for 8 h in a LB medium (pH 6.5) consisting of bactotryptone (10 g L^{-1}), yeast extract (5 g L^{-1}), and NaCl (10 g L^{-1}). After centrifugation of the cultured broth at 12,000 rpm for 10 min, the harvested cells were washed with physiological saline (NaCl, 7 g L^{-1}) and then suspended in physiological saline, resulting in a cell suspension of *E. coli*. The cell concentrations were determined using a calibration curve and turbidity quantified by the absorbance measured at 600 nm on an UV–Vis spectrometer [24].

2.6 PDI of *E. coli*

PDI of *E. coli* was performed as follows. A phosphate buffer (0.1 M, pH 7.6) was prepared by dissolving Na$_2$HPO$_4$ (2.469 g) and NaH$_2$PO$_4$ (0.312 g) in 100 mL of water. The suspension of *E. coli* cells (1 × 10^5 cells mL^{-1}, 1.0 mL), an aqueous solution of the studied sensitizers (25–100 μM, 0.1 mL), and the phosphate buffer (0.1 M, pH 7.6, 8.9 mL) were introduced into L-type glass tubes, resulting in a buffer solution (10 mL) containing *E. coli* (1 × 10^4 cells mL^{-1}) and the studied sensitizers (0.25–1.0 μM). Under dark conditions, the L-type glass tubes were set on a reciprocal shaker and shaken at 160 rpm at room temperature for 2 h [24]. And then the L-type glass tubes were irradiated using a fluorescent lamp (Panasonic FL-15ECW, Japan; wave length = 400–723 nm; the maximum intensity: 545 nm; 10.5 W cm^{-2}) on a reciprocal shaker at room temperature. A portion of the reaction mixture (0.1 mL) was taken up to 2 h at 20-min intervals and plated on LB plates. The LB plates were incubated for 30 h at 30°C.

The amount of the living cells (*B*) was defined as the average number of *E. coli* colonies that appeared after an incubation period of 30 h in three replicate plates. The *B* values for the PDI sensitizers were recorded at each irradiation time.
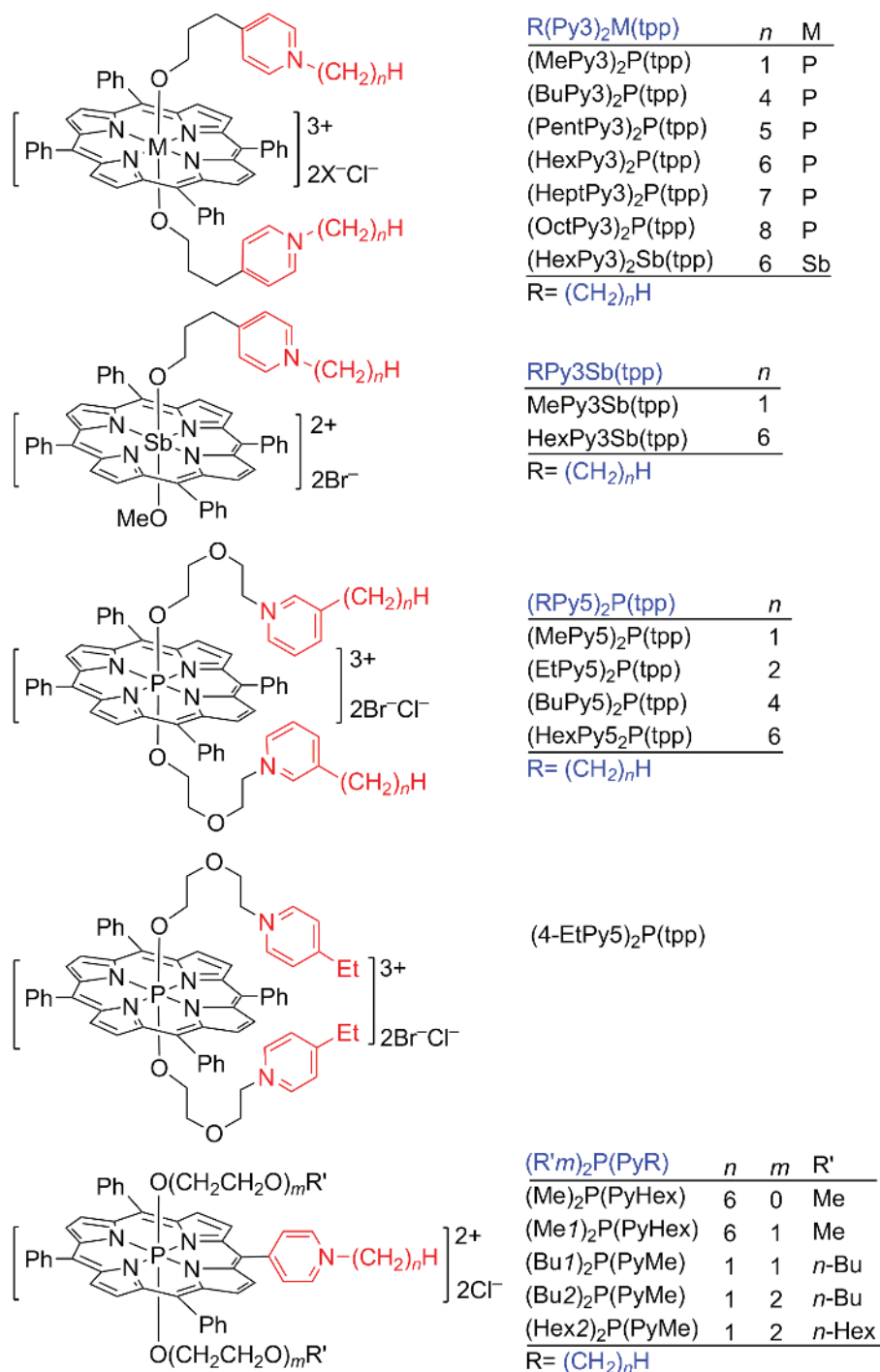
2.7 Fluorescence imaging

Incorporation of porphyrin sensitizers inside cells can be examined by fluorescence microscopy images of *E. coli* on a confocal laser scanning microscope (CLSM) under laser excitation at 543 nm. The aqueous solution containing the porphyrin sensitizers and *E. coli* was incubated for 3 h at 25°C. The concentrated solution was sandwiched between a cover slip and an agar pad on a bottom cover slip to maintain its position within the same focal plane [36].

3. Results

3.1 Properties of RPy-bonded P-porphyrins

Figure 2 shows the structures of the prepared porphyrins, which were water soluble due to cationic complexes. The water solubility (C_W) is listed in **Table 1**. In addition, **Table 1** lists the absorption coefficient (ε) of Soret band around 431 nm and Q-band at 562 nm in MeOH. These porphyrins could absorb strongly visible

R(Py3)$_2$M(tpp)	n	M
(MePy3)$_2$P(tpp)	1	P
(BuPy3)$_2$P(tpp)	4	P
(PentPy3)$_2$P(tpp)	5	P
(HexPy3)$_2$P(tpp)	6	P
(HeptPy3)$_2$P(tpp)	7	P
(OctPy3)$_2$P(tpp)	8	P
(HexPy3)$_2$Sb(tpp)	6	Sb
R= (CH$_2$)$_n$H		

RPy3Sb(tpp)	n
MePy3Sb(tpp)	1
HexPy3Sb(tpp)	6
R= (CH$_2$)$_n$H	

(RPy5)$_2$P(tpp)	n
(MePy5)$_2$P(tpp)	1
(EtPy5)$_2$P(tpp)	2
(BuPy5)$_2$P(tpp)	4
(HexPy5$_2$P(tpp)	6
R= (CH$_2$)$_n$H	

(4-EtPy5)$_2$P(tpp)

(R'm)$_2$P(PyR)	n	m	R'
(Me)$_2$P(PyHex)	6	0	Me
(Me1)$_2$P(PyHex)	6	1	Me
(Bu1)$_2$P(PyMe)	1	1	n-Bu
(Bu2)$_2$P(PyMe)	1	2	n-Bu
(Hex2)$_2$P(PyMe)	1	2	n-Hex
R= (CH$_2$)$_n$H			

Figure 2.
Polycationic P- and Sb-porphyrins bonded to alkylpyridinium (RPy).

light. Moreover, they could generate $^1O_2$ efficiently, since the quantum yields for the formation of $^1O_2$ were found to be 0.88 for $(HexPy3)_2P(Tpp)^{3+}$ and 0.87 for $(Bu2)_2P(MePyTpp)^{2+}$ [23].

3.2 Results of PDI of *E. coli*

Results of PDI of *E. coli* are summarized in **Table 2**. As seen from **Table 2**, *Meso*-RPy-substituted P-porphyrins $((R'm)_2P(RPyTpp)^{2+})$ have cytotoxicity, since *E. coli* was inactivated under dark conditions.

Based on **Table 2**, the survival ratios were calculated as $100B/B_0$ where B_0 is the initial amount of bacteria. From the time-course plots of survival ratios ($100B/B_0$), the half-life ($T_{1/2}$ in min), i.e., the time required to reduce B from B_0 to $0.5B_0$, was measured. A typical example of time-course plots is the case of PDI of *E. coli* by $(HexPy3)_2P(Tpp)^{3+}$ as shown in **Figure 3**. In this case, the $T_{1/2}$ value of

Sensitizers	[P]/ μM [b]	Amount of bacteria ([B])/CFU mL^{-1} [a]						
		t = 0/min [c]	20	40	60	80	100	120
$(MePy3)_2P(tpp)$	2.0	512 ± 22	450 ± 14	383 ± 13	344 ± 20	198 ± 13	103 ± 4.5	27 ± 1.2
$(BuPy3)_2P(tpp)$	2.0	377 ± 56	216 ± 10	105 ± 9.9	39 ± 5.3	18 ± 3.2	6.0 ± 2.7	2.3 ± 0.6
$(PentPy3)_2P(tpp)$	0.5	105 ± 12	65 ± 12	36 ± 4.6	19 ± 3.8	14 ± 4.0	11 ± 3.1	7.0 ± 2.0
$(HexPy3)_2P(tpp)$	0.5	243 ± 23	156 ± 5.2	125 ± 5.8	86 ± 3.1	77 ± 7.5	60 ± 1.2	17 ± 6.0
$(HeptPy3)_2P(tpp)$	0.4	203 ± 16	117 ± 9.1	53 ± 3.8	39 ± 3.1	15 ± 1.2	4.7 ± 2.1	3.0 ± 0
$(OctPy3)_2P(tpp)$	0.5	294 ± 14	215 ± 15	194 ± 12	136 ± 16	103 ± 9.9	76 ± 10	44 ± 8.0
$(HexPy3)_2Sb(tpp)$	1.0	152 ± 7.1	110 ± 4.7	76 ± 17	49 ± 4.2	36 ± 15	21 ± 4.5	45 ± 8.7
$(MePy3)Sb(tpp)$	1.0	170 ± 13	167 ± 17	134 ± 8.0	126 ± 6.8	102 ± 17	108 ± 26	113 ± 13
$(HexPy3)Sb(tpp)$	1.0	131 ± 28	120 ± 14	75 ± 11	55 ± 16	36 ± 11	23 ± 3.5	13 ± 1.7
$(MePy5)_2P(tpp)$	1.0	29 ± 6.4	16 ± 4.2	12 ± 5.6	10 ± 1.0	13 ± 2.3	6.7 ± 2.1	6.7 ± 1.5
$(EtPy5)_2P(tpp)$	0.25	167 ± 14	141 ± 18	59 ± 9.0	5.7 ± 0.6	1.7 ± 1.5	0.3 ± 0.6	0
$(BuPy5)_2P(tpp)$	0.25	145 ± 11	123 ± 7.6	92 ± 7.5	63 ± 4.6	33 ± 8.4	6.7 ± 4.9	4.7 ± 0.6
$(HexPy5)_2P(tpp)$	0.25	213 ± 10	213 ± 9.5	176 ± 16	166 ± 6.8	140 ± 8.2	132 ± 12	97 ± 4.4
$(4-EtPy5)_2P(tpp)$	0.5	139 ± 14	85 ± 13	88 ± 16	62 ± 6.0	42 ± 8.7	32 ± 7.0	33 ± 1.5
$(Me)_2P(PyHex)$	2.0	90 ± 13	88 ± 17	49 ± 7.8	27 ± 6.2	17 ± 5.1	13 ± 1.5	15 ± 3.1
$(Me1)_2P(PyHex)$	0.5	89 ± 2.7	57 ± 2.9	42 ± 7.2	18 ± 3.5	16 ± 2.9	8.3 ± 4.0	5.7 ± 1.2
$(Me1)_2P(PyHex)$ [d]	0.5	109 ± 26	99 ± 13	59 ± 12	64 ± 10	65 ± 165	59 ± 42	41 ± 9.6
$(Bu1)_2P(PyMe)$	0.5	24 ± 3.6	20 ± 4.5	13 ± 3.0	12 ± 1.2	7.3 ± 2.9	3.7 ± 2.1	4.7 ± 1.2
$(Bu1)_2P(PyMe)$ [d]	0.5	34 ± 5.0	25 ± 3.5	28 ± 6.1	31 ± 3.5	25 ± 1.5	20 ± 2.7	19 ± 2.1
$(Bu2)_2P(PyMe)$	2.0	126 ± 14	56 ± 3.8	21 ± 4.9	8.7 ± 2.1	3.3 ± 3.5	1.7 ± 0.6	2.3 ± 2.1
$(Bu2)_2P(PyMe)$ [d]	2.0	150 ± 13	141 ± 5.5	129 ± 8.3	124 ± 11	116 ± 13	84 ± 14	94 ± 12
$(Hex2)_2P(PyMe)$	1.0	63 ± 5.9	50 ± 7.5	56 ± 2.1	45 ± 8.1	39 ± 9.1	35 ± 6.1	33 ± 12

[a]*PDI of E. coli was performed in a phosphate buffer solution (10 mL, pH 7.6) containing E. coli (ca. 2×10^4 cell mL^{-1}) and porphyrin sensitizers under the irradiation of a fluorescent lamp. CFU = colony formation unit.*
[b]*[P] was adjusted to attain the value of $T_{1/2}$ between 20 and 120 min.*
[c]*Irradiation time (t) in min.*
[d]*Under dark conditions.*

Table 2.
PDI of E. coli with cationic porphyrins under visible light irradiation.
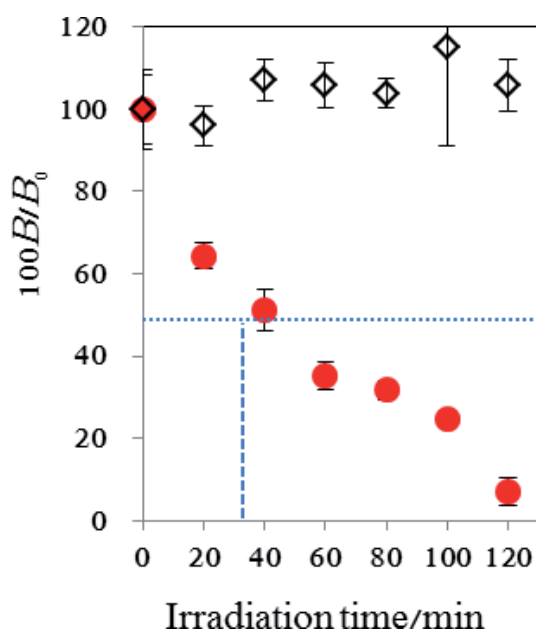
Figure 3.
Typical example of time-course plots of survival ratio ($100B/B_0$) in the PDT of E. coli with $(HexPy3)_2P(Tpp)^{3+}$ (0.5 μM) under visible light irradiation (•) and under dark conditions (◇). The $T_{1/2}$ was determined to be 31 min from the plots.

$(HexPy3)_2P(Tpp)^{3+}$ was determined to be 31 min. The minimum concentrations of the sensitizer $[P]$ were adjusted such that $T_{1/2}$ attained values between 20 and 120 min. Thus, the bactericidal activity (A_F in $\mu M^{-1} h^{-1}$) was evaluated using the following equation: $A_F = 60/([P] \times T_{1/2})$. **Table 3** summarizes $[P]$ and A_F values in the PDI of *E. coli*.

3.3 PDI activity of the porphyrin sensitizers toward *E. coli*

As shown in **Table 3**, the A_F values were dependent on the number of carbon atoms (n) in the alkyl group on the RPy group in $(RPy3)_2M(Tpp)^{3+}$ (M = P, Sb), $RPy3Sb(Tpp)^{2+}$, and $(RPy5)_2P(Tpp)^{3+}$. **Figure 4A** shows the dependence of the A_F values on n in the case of a series of $(RPy3)_2M(Tpp)^{3+}$ (M = P, Sb) and $RPy3Sb(Tpp)^{2+}$. The maximum value of A_F appeared at $n = 7$ whose $[P]$ value was 0.40 μM. Moderately long alkyl chain made the sensitizer more active toward *E. coli* [24]. In the case of a series of $(RPy5)_2P(Tpp)^{3+}$ (**Figure 4B**), the maximum value of A_F appeared at $n = 2$ whose $[P]$ value for *E. coli* was 0.25 μM [25]. Therefore, the A_F and $[P]$ values of 3-ethyl analog were compared with those of 4-ethyl isomer. It was found that the A_F value of 4-ethyl isomer was lower than that of 3-ethyl isomer. In the case of the 4-ethyl analog, broadening of Soret and Q bands occurred due to aggregation of porphyrin chromophores. It is suggested that aggregation caused to lower the A_F value of 4-ethyl isomer $(4EtPy5)_2P(Tpp)^{3+}$.

Figure 5 shows the fluorescence images of *E. coli* in the presence of depicting the emission from $(MePy3)_2P(Tpp)^{3+}$ and $(HexPy3)_2P(Tpp)^{3+}$ inside *E. coli*. The images show that $(HexPy3)_2P(Tpp)^{3+}$ was accumulated inside *E. coli*, whereas $(MePy3)_2P(Tpp)^{3+}$ was not. $(HexPy3)_2P(Tpp)^{3+}$, which had a large affinity to *E. coli*, had the high PDI activity. The RPy group with a long alkyl chain made the sensitizer reactive toward *E. coli*.

Sensitizer[a]	Z[b]	Metal	n[c]	$[P]/\mu M$[d]	$T_{1/2}/min$[e]	$A_F/\mu M^{-1} h^{-1}$[f]
(MePy3)$_2$P(tpp)	+3	P	1	2.0	66	0.5
(BuPy3)$_2$P(tpp)	+3	P	4	2.0	27	1.1
(PentPy3)$_2$P(tpp)	+3	P	5	0.5	29	4.1
(HexPy3)$_2$P(tpp)	+3	P	6	0.5	31	3.8
(HeptPy3)$_2$P(tpp)	+3	P	7	0.4	24	6.3
(OctPy3)$_2$P(tpp)	+3	P	8	0.5	63	1.9
(HexPy3)$_2$Sb(tpp)	+3	Sb	6	1.0	36	1.7
(MePy3)Sb(tpp)	+2	Sb	1	1.0	106	0.6
(HexPy3)Sb(tpp)	+2	Sb	6	1.0	68	0.9
(MePy5)$_2$P(tpp)	+3	P	1	1.0	40	1.5
(EtPy5)$_2$P(tpp)	+3	P	2	0.25	32	7.5
(ButPy5)$_2$P(tpp)	+3	P	4	0.25	53	4.5
(HexPy5)$_2$P(tpp)	+3	P	6	0.25	120	2.0
(4EtPy5)$_2$P(tpp)	+3	P	2	0.5	50	2.4
(Me)$_2$P(PyHex)	+2	P	6	2.0	45	0.7
(Me1)$_2$P(PyHex)	+2	P	6	0.5	37	3.2
(Bu1)$_2$P(PyMe)	+2	P	1	0.5	55	2.2
(Bu2)$_2$P(PyMe)	+2	P	1	2.0	23	1.3
(Hex2)$_2$P(PyMe)	+2	P	1	1.0	116	0.5

[a]The PDI did not occur under dark conditions except for meso-RPy-substituted P-porphyrins, which were cytotoxic under dark conditions

[b]Z = charge of the complex.

[c]n = carbon number of the alkyl chain on the AP.

[d]$[P]$ = minimum concentrations of the porphyrins adjusted to attain the value of $T_{1/2}$ between 20 and 120 min.

[e]$T_{1/2}$ = half-life in min.

[f]A_F = PDI activity in $\mu M^{-1} h^{-1}$: $A_F = 60/([P] \times T_{1/2})$.

Table 3.
The $[P]$, $T_{1/2}$, and A_F values in the PDI of E. coli by cationic porphyrins.

## 3.4 Comparison of the PDI activity in *E. coli* with the PDI activity in *Saccharomyces cerevisiae*

For comparison of the PDI activity in *E. coli* and other microorganisms, PDI of *S. cerevisiae* was performed using (RPy3)$_2$P(Tpp)$^{3+}$. It could photoinactivate *S. cerevisiae* in lower concentration compared with the case of *E. coli* [23]. For example, the $[P]$ values of (MePy3)$_2$P(Tpp)$^{3+}$ for *S. cerevisiae* were 0.05 μM, while that for *E. coli* was 2.0 μM. Moreover, PDI of *S. cerevisiae* was performed using other porphyrins (Type E, **Figure 6**), which were monocationic and highly hydrophobic. The PDI of *S. cerevisiae* occurred efficiently by Type E porphyrins [37]. The $[P]$ values for the PDI of *S. cerevisiae* were optimized to be 0.005 μM. Thus, *S. cerevisiae* has low drug resistance for hydrophobic sensitizers rather than polycationic sensitizers, since the $[P]$ value of tricationic porphyrins was larger than that of monocationic porphyrins (Type E). On the contrary, no PDI of *E. coli* by Type E porphyrins occurred at all. This result shows that a more positive character is required for an efficient PDI of *E. coli*.
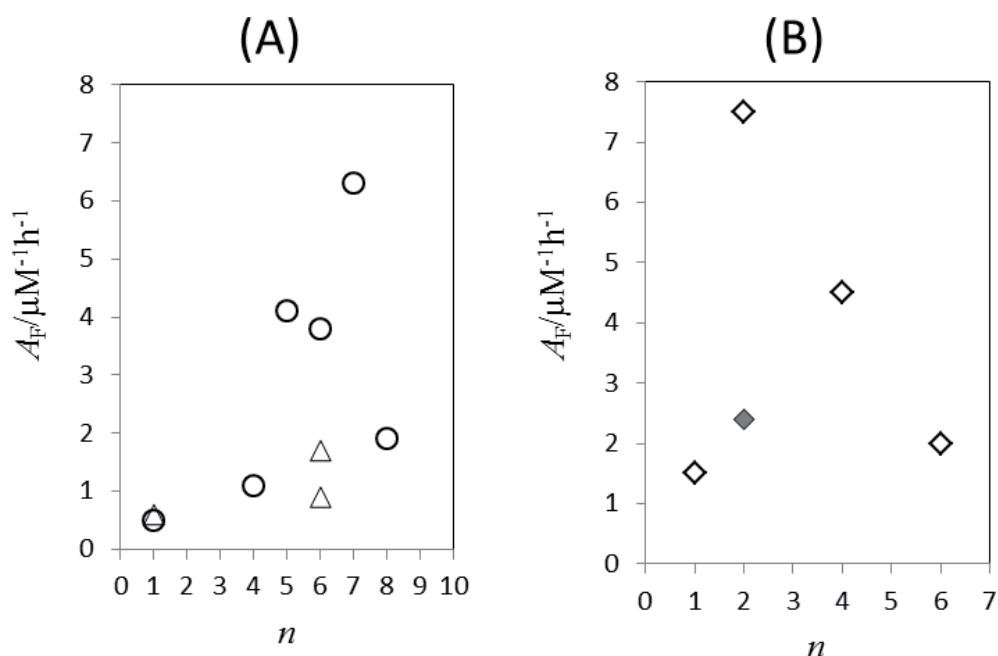
Figure 4.
Relationship between the A_F values and number of carbon atoms (n) in the alkyl group on the alkylpyridinium (RPy) in PDI of E. coli using (A) P-porphyrins ($(RPy3)_2P(Tpp)^{3+}$, ○) and Sb-porphyrins ($(RPy3)_2Sb(Tpp)^{3+}$ and $RPy3Sb(Tpp)^{2+}$, △) and (B) 3-alkyl-substituted P-porphyrins ($(RPy5)_2P(Tpp)^{3+}$, ◇) and their 4-ethyl-analog ($(4EtPy5)_2P(Tpp)^{3+}$, ◆).
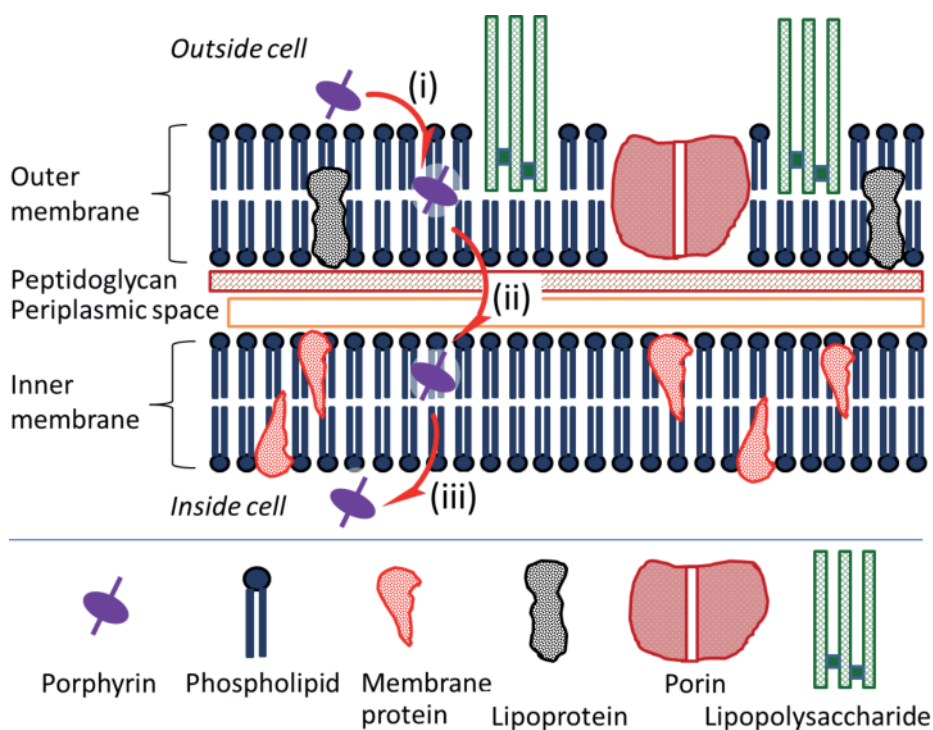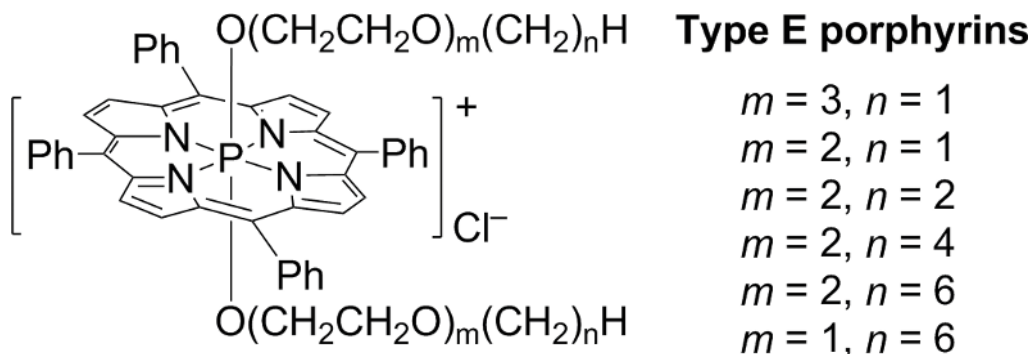

Figure 5.
The incorporation of porphyrins inside bacteria through self-promoted mechanism. (i) Cationic porphyrin adsorbs to the anionic outer membrane; (ii) amphiphilic porphyrin interacts with hydrophobic parts of outer and inner membranes; (iii) porphyrin is incorporated inside the cell.
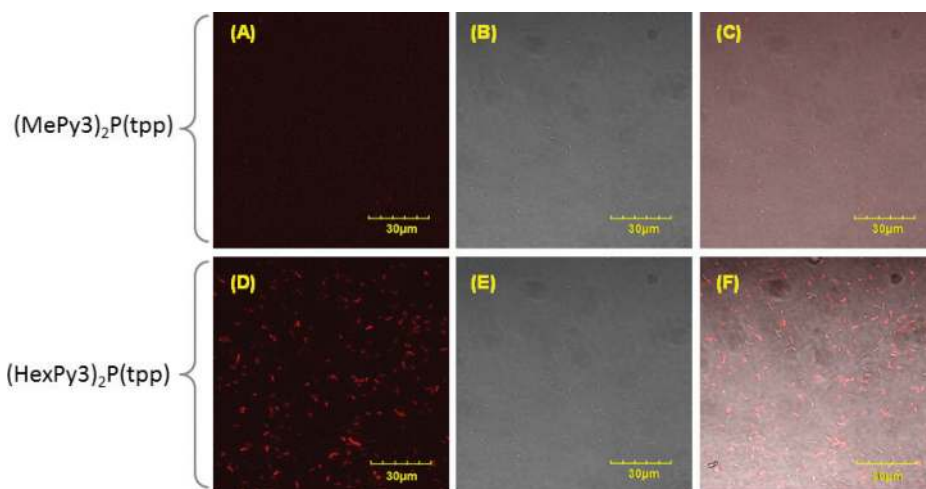
Figure 6.
Fluorescence images of E. coli obtained with a CLSM under laser-excitation at 543 nm. Fluorescence coming from inside the cells was observed with the addition of (HexPy3)₂P(Tpp)³⁺ (D), but not observed with the addition of (MePy3)₂P(Tpp)³⁺ (A). Transmission images of E. coli containing (HexPy3)₂P(Tpp)³⁺ (E) and (MePy3)₂P(Tpp)³⁺ (B). The image of C is obtained by overlapping images in A and B, and the image in F is obtained by overlapping images in D and E.

4. Discussion

The mechanism behind the PDI activity in *E. coli* is still not completely understood. However, it is known that the first contact of porphyrin photosensitizers occurs at the outer membrane. The outer leaflet of the outer membrane mainly consists of lipopolysaccharides and phospholipids, which are negatively charged and are stabilized with divalent cations such as Ca^{2+} and Mg^{2+} [38]. Therefore, electrostatic interaction between cationic photosensitizers and the outer leaflet instead of these divalent cations promotes destabilization of the outer membrane [39]. In the case of the cationic porphyrins with hydrophobic character, or the amphiphilic one, they can also interact with not only the outer leaflet but also the inner leaflet of the outer membrane and the plasma membrane (**Figure 7**). Thus, the amphiphilic porphyrins may be incorporated inside *E. coli* cells via the self-promoted uptake pathway [37]. The porphyrin

Figure 7.
P-porphyrins (Type E) substituted with alkylethyleneglycol ligands.

sensitizers passed through the cell wall may reach biogenic proteins, lipids, and DNA. Under irradiation, reactive oxygen such as $^1O_2$ was generated near to these molecules to induce cell death. Although E-type porphyrins generate $^1O_2$ efficiently under visible light irradiation, the lifetime of $^1O_2$ in aqueous medium is very short (~3 μs) [40]. Thus, for efficient PDI, $^1O_2$ should be generated as close as possible to the target molecules. The P type porphyrins with amphiphilic characters, which can be incorporated inside *E. coli*, will be advantageous to PDI via $^1O_2$ generation.

5. Conclusion

PDI of *E. coli* K-12 (IFO 3301) was examined using 19 kinds of cationic porphyrin sensitizers. In conclusion, (1) *E. coli* has high drug-resistance toward the hydrophobic and monocationic porphyrins such as Type E. (2) However, *E. coli* has low drug-resistance toward polycationic porphyrins such as Type P. (3) Especially, *E. coli* has low drug-resistance toward polycationic porphyrins with moderately long alkyl chain, for example, $(HeptPy3)_2P(Tpp)^{3+}$ and $(EtPy5)_2P(Tpp)^{3+}$. Alkyl chains might result in moderate hydrophobicity to take advantage of interaction between hydrophobic parts of cell membranes. (4) Polycationic porphyrins can interact with the anionic outer membrane at the first step and DNA and proteins inside the cells with strong binding affinities.

Acknowledgements

Conflict of interest

The authors declare that they have no competing interests.

Abbreviations

A_F	PDI activity (in $\mu M^{-1} h^{-1}$): $A_F = 60/([P] \times T_{1/2})$
B	mount of bacteria
B_0	initial amount of bacteria
CFU	colony formation unit
C_W	water solubility
ε	molar absorption coefficient
LB	Luria-Bertani medium
m	number of ethylene glycol unit
n	carbon number of the alkyl chain on the Ap
$[P]$	minimum effective concentrations of sensitizer
PDI	photodynamic inactivation
RPy	*N*-alkylpyridinium group
t	irradiation time
$T_{1/2}$	half-life time required to reduce B from B_0 to $0.5B_0$
Z	valence number of the porphyrin complex

Abbreviations of substances

$(Br5)_2P(Tpp)^+$	bis(5-bromo-3-oxapentyloxo)tetraphenylporphyrinato-phosphorus chloride
$(Py3)_2P(Tpp)^+$	bis[3-(4-pyridyl)propoxo]tetraphenylporphyrinato-phosphorus chloride
$(Py3)_2Sb(Tpp)^+$	bis[3-(4-pyridyl)propoxo]tetraphenylporphyrinato-antimony bromide
$Py3Sb(Tpp)^+$	3-(4-Pyridyl)propoxo(methoxo)tetraphenylporphyrinato antimony bromide
PyTpp	triphenyl(4-pyridinyl)porphyrin
$(RPy3)_2P(Tpp)^{3+}$	bis[3-(1-alkyl-4-pyridinio)propoxo]tetraphenylpor-phyrinatophosphorus chloride, dihalide
$(RPy3)_2Sb(Tpp)^{3+}$	bis[3-(1-alkyl-4-pyridinio)propoxo]tetraphenylpor-phyrinatoantimony tribromide
$(RPy5)_2P(Tpp)^{3+}$	bis[5-(3-alkyl-1-pyridinio)-3-oxapentyloxo]tetraphenyl-porphyrinatophosphorus dibromide, chloride
$RPy3Sb(Tpp)^{2+}$	α-(methoxo)-β-[3-(1-hexyl-4-pyridinio)-1-propoxo]-5,10,15,20-tetraphenylporphyrinatoantimony (V) dibromide
$(R'm)_2P(RPyTpp)^{2+}$	bis(2-alkyloxyethoxo)-5-(1-alkyl-4-pyridinio)-10,15,20-triphenylporphyrinatophosphorus (V) dichloride
TMP	*meso*-tetra[4-(1-methylpyridinium)]porphyrin

Author details

Jin Matsumoto[1], Tomoko Matsumoto[2], Kazuya Yasuda[3] and Masahide Yasuda[1*]

1 Department of Applied Chemistry, Faculty of Engineering, University of Miyazaki, Miyazaki, Japan

2 Center for Collaborative Research and Community Cooperation, University of Miyazaki, Miyazaki, Japan

3 Department of Pharmacy, University of Miyazaki Hospital, Miyazaki, Japan

*Address all correspondence to: yasuda@cc.miyazaki-u.ac.jp

IntechOpen

References

[1] Castano AP, Demidova TN, Hamblin MR. Mechanisms in photodynamic therapy: Part one—Photosensitizers, photochemistry and cellular localization. Photodiagnosis and Photodynamic Therapy. 2004;**1**:279-293

[2] Hamblin MR, Hasan T. Photodynamic therapy: A new antimicrobial approach to infectious disease? Photochemical and Photobiological Sciences. 2004;**3**:436-450

[3] Salmon-Divon Nitzan MY, Malik Z. Mechanistic aspects of *Escherichia coli* photodynamic inactivation by cationic tetra-*meso*(*N*-methylpyridyl)porphine. Photochemical and Photobiological Sciences. 2004;**3**:423-429

[4] Banfi S, Caruso Buccafurni EL, Battini V, Zazzaron S, Barbieri P, Orlandi V. Antibacterial activity of tetraarylporphyrin photosensitizers: An in vitro study on gram negative and gram positive bacteria. Journal of Photochemistry and Photobiology, B: Biology. 2006;**85**:28-38

[5] Alves E, Faustino MAF, Neves MGPMS, Cunha T, Nadais H, Almeida A. Potential applications of porphyrins in photodynamic inactivation beyond the medical scope. Journal of Photochemistry and Photobiology C: Photochemistry Reviews. 2014;**22**:34-57

[6] Clifton CE. Photodynamic action of certain dyes on the inactivation of Staphylococcus bacteriophage. Proceedings of the Society for Experimental Biology and Medicine. 1931;**28**:745-746

[7] Perdrau JR, Todd C. The photodynamic action of methylene blue on bacteriophage. Proceedings of the Royal Society of London Series B, Containing Papers of a Biological Character. 1933;**112**:277-287

[8] Pandey RK, Zheng G. Porphyrins as photosensitizers in photodynamic therapy. In: Kadish KM, Smith KM, Guilluy R, editors. The Porphyrin Handbook. Vol. 6. San Diego: Academic Press; 2000. pp. 157-230

[9] Nyman ES, Hynninen PH. Research advances in the use of tetrapyrrolic photosensitizers for photodynamic therapy. Journal of Photochemistry and Photobiology B: Biology. 2004;**73**:1-28

[10] Shiragami T, Matsumoto J, Inoue H, Yasuda M. Antimony porphyrin complexes as visible-light driven photocatalyst. Journal of Photochemistry and Photobiology C Photochemistry Reviews. 2005;**6**:227-248

[11] Ethirajan M, Chen Y, Joshi P, Pandey RK. The role of porphyrin chemistry in tumor imaging and photodynamic therapy. Chemical Society Reviews. 2011;**40**:340-362

[12] Kalyanasundaram K. Photochemistry of water-soluble porphyrins: Comparative study of isomeric tetrapyridyl- and tetrakis (*N*-methylpyridiniumyl)porphyrins. Inorganic Chemistry. 1984;**23**:2453-2459

[13] Girek B, Sliwa W. Porphyrins functionalized by quaternary pyridinium units. Journal of Porphyrins and Phthalocyanines. 2013;**17**:1139-1156

[14] Ben Amor T, Bortolotto L, Jori G. Porphyrins and related compounds as photoactivatable insecticides. 2. Phototoxic activity of meso-substituted porphyrins. Photochemistry and Photobiology. 1998;**68**:314-318

[15] Kano K, Fukuda K, Wakami H, Nishiyabu R, Pasternack RF. Factors influencing self-aggregation tendencies of cationic porphyrins in aqueous

solution. Journal of the American Chemical Society. 2000;**122**:7494-7502

[16] Kubát P, Lang K, Anzenbacher P Jr, Jursíková K, Král V, Ehrenberg B. Interaction of novel cationic *meso*-tetraphenylporphyrins in the ground and excited states with DNA and nucleotides. Journal of the Chemical Society, Perkin Transactions. 2000;**1**:933-941

[17] Trommel JS, Marzilli LG. Synthesis and DNA binding of novel water-soluble cationic methylcobalt porphyrins. Inorganic Chemistry. 2001;**40**:4374-4383

[18] Lang K, Mosinger J, Wagnerová DM. Photophysical properties of porphyrinoid sensitizers non-covalently bound to host molecules; models for photodynamic therapy. Coordination Chemistry Reviews. 2004;**248**:321-350

[19] Banfi S, Caruso E, Buccafurni L, Battini V, Zazzaron S, Barbieri P, et al. Antibacterial activity of tetraaryl-porphyrin photosensitizers: An in vitro study on gram negative and gram positive bacteria. Journal of Photochemistry and Photobiology B: Biology. 2006;**85**:28-38

[20] Haeubl M, Reith LM, Gruber B, Karner U, Müller N, Knör G, et al. DNA interactions and photocatalytic strand cleavage by artificial nucleases based on water-soluble gold(III) porphyrins. Journal of Biological Inorganic Chemistry. 2009;**14**:1037-1052

[21] Batinic-Haberle I, Spasojevic I, Tse HM, Tovmasyan A, Rajic Z, Clair DKS, et al. Design of Mn porphyrins for treating oxidative stress injuries and their redox-based regulation of cellular transcriptional activities. Amino Acids. 2012;**42**:95-113

[22] Matsumoto J, Kubo T, Shinbara T, Matsuda N, Shiragami T, Fujitsuka M, et al. Spectroscopic analysis of the interaction of human serum albumin with tricationic phosphorus porphyrins bearing axial pyridinio groups. Bulletin of the Chemical Society of Japan. 2013;**86**:1240-1247

[23] Matsumoto J, Kai Y, Yokoi H, Okazaki S, Yasuda M. Assistance of human serum albumin to photo-sensitized inactivation of *Saccharomyces cerevisiae* with axially pyridinio-bonded P-porphyrins. Journal of Photochemistry and Photobiology B: Biology. 2016;**161**:279-283

[24] Matsumoto J, Suemoto Y, Kanemaru H, Takemori K, Shigehara M, Miyamoto A, et al. Alkyl substituent effect on photosensitized inactivation of *Escherichia coli* by pyridinium-bonded P-porphyrins. Journal of Photochemistry and Photobiology B: Biology. 2017;**168**:124-131

[25] Matsumoto J, Yasuda M. Optimal axial alkylpyridinium-bonded tricationic P-porphyrin in photodynamic inactivation of *Escherichia coli*. Medicinal Chemistry Research. 2018;**27**:1478-1484

[26] Matsumoto J, Shiragami T, Hirakawa K, Yasuda M. Water-solubilization of P(V) and Sb(V) porphyrin and their photobiological application. International Journal of Photoenergy. 2015:148964

[27] Pasternack RF, Ewen S, Rao A, Meyer AS, Freedman MA, Collings PJ, et al. Interactions of copper(II) porphyrins with DNA. Inorganica Chimica Acta. 2001;**317**:59-71

[28] Sirish M, Chertkov VA, Schneider HJ. Porphyrin-based peptide receptors: Syntheses and NMR analysis. Chemistry—A European Journal. 2002;**8**:1181-1188

[29] Marczak R, Sgobba V, Kutner W, Gadde S, D'Souza F, Guldi DM. Langmuir-Blodgett films of a

cationic zinc porphyrin-imidazole-functionalized fullerene dyad: Formation and photoelectrochemical studies. Langmuir. 2007;**23**:1917-1923

[30] Tada-Oikawa S, Oikawa S, Hirayama J, Hirakawa K, Kawanishi S. DNA damage and apoptosis induced by photosensitization of 5,10,15,20-tetrakis (*N*-methyl-4-pyridyl)- 21H,23H-porphyrin via singlet oxygen generation. Photochemistry and Photobiology. 2009;**85**:1391-1399

[31] Kim YH, Jung SD, Lee MH, Im C, Kim YH, Jang YJ, et al. Photoinduced reduction of manganese(III) *meso-*tetrakis(1-methyl-pyridinium-4-yl) porphyrin at AT and GC base pairs. The Journal of Physical Chemistry. B. 2013;**117**:9585-9590

[32] Gyulkhandanyan A, Gyulkhandanyan L, Ghazaryan R, Fleury F, Angelini M, Gyulkhandanyan G, et al. Assessment of new cationic porphyrin binding to plasma proteins by planar microarray and spectroscopic methods. Journal of Biomolecular Structure and Dynamics. 2013;**31**:363-375

[33] Fueda Y, Suzuki H, Komiya Y, Asakura Y, Shiragami T, Matsumoto J, et al. Bactericidal effect of silica gel-supported porphyrinatophosphorus(V) catalysts on *Escherichia coli* under visible light irradiation. Bulletin of the Chemical Society of Japan. 2006;**79**:1420-1425

[34] Shiragami T, Andou Y, Hamasuna Y, Yamaguchi F, Shima K, Yasuda M. Effects of an axial ligands on reduction potentials, proton dissociation, and fluorescence quantum yield of hydroxoporphyrinatoantimony(V) complexes. Bulletin of the Chemical Society of Japan. 2002;**75**:1577-1582

[35] Shiragami T, Tanaka K, Andou Y, Tsunami S, Matsumoto J, Luo H, et al. Synthesis and spectroscopic analysis of tetraphenylporphyrinatoantimony(V) complexes linked to boron-dipyrrin chromophore on axial ligands. Journal of Photochemistry and Photobiology A: Chemistry. 2005;**170**:287-297

[36] Tanaka K, Kitamura E, Tanaka TU. Live-cell analysis of kinetochore-microtubule interaction in budding yeast. Methods. 2010;**51**:206-213

[37] Matsumoto J, Shinbara T, Tanimura S, Matsumoto T, Shiragami T, Yokoi H, et al. Water-soluble phosphorus porphyrins with high activity for visible light-assisted inactivation of *Saccharomyces cerevisiae*. Journal of Photochemistry and Photobiology A: Chemistry. 2018;**218**:178-184

[38] Wang X, Quinn PJ. Lipopolysaccharide: Biosynthetic pathway and structure modification. Progress in Lipid Research. 2010;**49**:97-107

[39] Minnock A, Vernon DI, Schofield J, Griffiths J, Parish JH, Brown SB. Mechanism of uptake of a cationic water-soluble pyridinium zinc phthalocyanine across the outer membrane of *Escherichia coli*. Antimicrobial Agents and Chemotherapy. 2000;**44**:522-527

[40] Uzdensky AB. The biophysical aspects of photodynamic therapy. Biophysics. 2016;**61**:547-557